



## Design of Air Break Nut Used in Dishwasher Based on Fracture Behavior

### Bulaşık Makinesinde Kullanılan Su Cebi Somununun Kırılma Davranışı Tabanlı Tasarımı

Furkan Kılavuz <sup>1,2</sup>, Halil Sayır <sup>2</sup>, Binnur Gören Kırıl <sup>3\*</sup>

<sup>1</sup> Dokuz Eylül University, The Graduate School of Natural and Applied Sciences, Izmir, TURKEY

<sup>2</sup> Vestel White Goods Co., Manisa, TURKEY

<sup>3</sup> Dokuz Eylül University, Faculty of Engineering, Department of Mechanical Engineering, Izmir, TURKEY

Sorumlu Yazar / Corresponding Author \*: binnur.goren@deu.edu.tr

Geliş Tarihi / Received: 11.07.2019

Kabul Tarihi / Accepted: 09.08.2019

Araştırma Makalesi/Research Article

DOI: 10.21205/deufmd.2020226424

*Atıf şekli/ How to cite:* KILAVUZ, F., SAYIR, H., GÖREN-KIRAL, B. (2020). Design of Air Break Nut Used in Dishwasher Based on Fracture Behavior. DEUFMD 22(64),247-257.

#### Abstract

Air break part used in dishwashers serves three main purposes. First, it measures the washing water by means of a flowmeter provided in the air break inlet. Second, it divides the washing water into two parts; one part is sent directly to the tub and the other part is sent to the water softening system. Third, static pressure needed in the salt-resin regeneration cycle is provided by the water filled into the air break tank. Air break part is assembled to the dishwasher tub using bolt and nut connection. During the assembly, crack initiation and propagation are observed in the air break nut. In this paper, mechanical behavior of the air break nut during the assembly is investigated by the structural and fracture analyses using the finite element method. Alternative designs for the air break nut are developed and compared with the current design in order to examine the effect of its design on the stress distribution and fracture behavior.

**Keywords:** Dishwasher, air break nut, fracture, finite element analysis.

#### Öz

Bulaşık makinelerinde kullanılan su cebi parçası üç ana amacı yerine getirir. Birincisi, yıkama suyunu, su cebi girişinde sağlanan bir debimetre vasıtasıyla ölçer. İkincisi, yıkama suyunu iki parçaya böler; bir kısım doğrudan küvete, diğer kısım su yumuşatma sistemine gönderilir. Üçüncüsü, tuz reçinesi rejenerasyon döngüsünde ihtiyaç duyulan statik basınç, su cebi tankına doldurulan su ile sağlanır. Su cebi parçası, civata ve somun bağlantısı kullanılarak bulaşık makinesinin küvetine monte edilir. Montaj esnasında, su cebi somununda çatlak oluşumu ve ilerlemesi gözlenmektedir. Bu makalede, sonlu elemanlar yöntemi kullanılarak yapısal ve kırılma analizleri ile su cebi somununun mekanik davranışı incelenmektedir. Su cebi somunu için alternatif tasarımlar geliştirilmiş ve tasarımların gerilme dağılımı ve kırılma davranışı üzerindeki etkisini incelemek üzere mevcut tasarımla karşılaştırılmıştır.

**Anahtar Kelimeler:** Bulaşık makinesi, su cebi somunu, kırılma, sonlu elemanlar analizi

## 1. Introduction

Failure of solids and structures may occur in various forms. Fracture mechanics deals with failure of solids caused by crack initiation and propagation. Fracture is the ultimate continuum of a material. Applied stress, crack length, and fracture toughness are three important factors in fracture mechanics. There are two basic approaches to establish fracture criteria, or crack propagation criteria: crack tip stress field and energy balance approaches. The fracture behavior of the solids and structures can be investigated analytically, numerically and experimentally. Fracture mechanics is used to evaluate the strength of a structure or component in the presence of a crack or flaw. It is the field of mechanics concerned with the study of propagation of cracks in materials. It uses methods of analytical solid mechanics to characterize the material's resistance of fracture [1].

Kubiak et al. examined the causes of fracture in a stream turbine blade root numerically [2]. They carried out turbine flow analysis together with verification of the blade root dimensions and tolerances and realized the natural frequencies and vibration modes analysis of the four blade group and the stress analysis of a blade using ANSYS. In the manuscript, the maximum stress at the vicinity of the crack was defined. For the determination of the static and dynamic stresses the dynamic and static steam forces were calculated. Urquiza et al. investigated the failure analysis of a 105MW Kaplan turbine auxiliary shaft from a hydropower plant. In order to determine the cause of failure, finite element analysis (FEA) was done to calculate the stress level under the maximum and minimum turbine blade inclination position in this study [3]. Karalis et al. investigated the causes of failure of a mechanical fastener obtained from a flange of a large-diameter steel tube operating in marine environment. Macrofractography and microfractography, standard optical metallography, scanning electron microscopy (SEM), X-ray fluorescence (XRF) and energy-dispersive X-ray spectroscopy techniques as well as numerical modeling were employed [4].

The present study aims to examine the stress distributions occurred in the air break nut which is a member of water softening system in dishwasher during the assembly using ANSYS Workbench 17.0 software [5]. In the study, the causes of the fracture of air break nut which rarely occurs on the assembly line are also

investigated. Principal stress distributions obtained by performing the finite elements method are examined as the material of the nut is brittle. Stress intensity factor values obtained by the finite element analysis are compared with fracture toughness of the material used for the nut to decide whether the fracture occurs or not. Critical crack length and critical torque values which the operator should apply to the nut in the assembly stage are determined considering the results obtained by the fracture analysis. Current nut design is also compared to new nut designs to see the effect of the geometry on the stress distributions and fracture behavior.

## 2. Material and Method

The air break part of the dishwasher plays an important role in the water softening system. This system consists of water inlet valve, salt container and air break nut. Air break nut examined in this study is shown in Figure 1. The water inlet passes through the flowmeter and passes through the air break part. The teeth crossed tightly in the region where the part is mounted. After the assembly of the air break nut, opening from the sharp edge towards the outside is occurred. It is observed that the fracture initiates from its sharp corner.

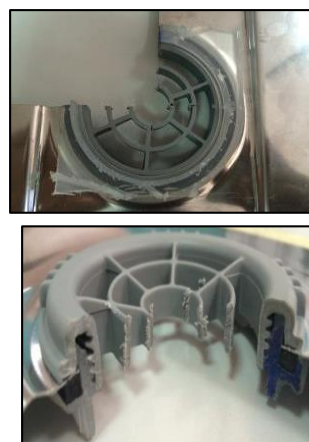


**Figure 1.** Air break nut

During the stage of the assembly of the air break nut, operator assembles the air break nut tightening it using an apparatus. The operator installs the nut by means of perpendicular force applied to the nut by the apparatus. Approximate values of applied torque is determined as 16 N·m. Figure 2 shows the three dimensional solid models of nut and apparatus modeled by Creo PTC 2.0 software.

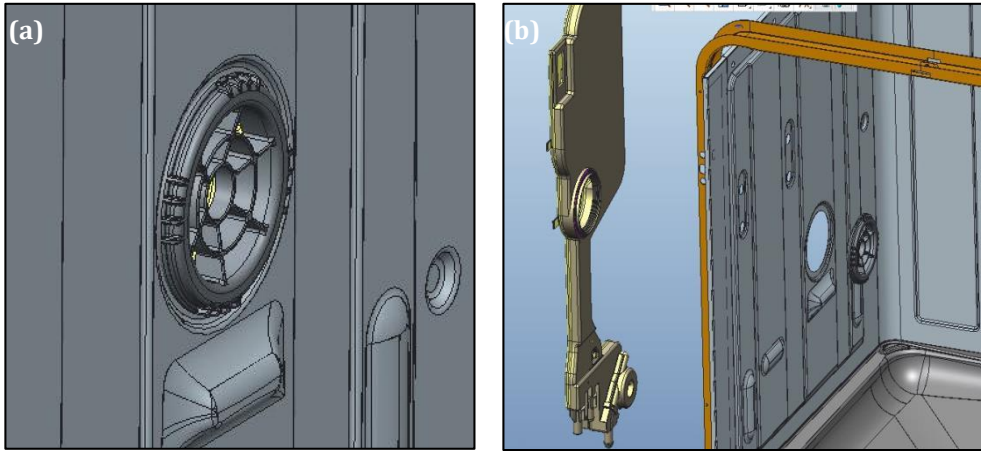


**Figure 2.** Three-dimensional model of (a) assembled of air break nut, (b) its apparatus

In application of assembling, a crack formation was observed at the edge of the nut as shown in Figure 3. It is seen that the crack progresses from the sharp corner. In this study, the current nut design and its improved new designs are examined to prevent or to minimize crack formation.



**Figure 3.** The region where crack formation was observed

### 3. Numerical Modeling

In this study, air break nut used in the dishwasher is modeled by using PTC Creo 2.0 software. Figure 4 shows the three dimensional solid model of the air break nut and its finite element model. Three-dimensional finite element analyses are carried out using ANSYS Workbench finite element program to examine the mechanical behavior of the air break nut under the loading.

As the first analysis, stress distribution in the present air break nut subjected to the static loading is examined. Then, the stress intensity factors for various crack length values are obtained to determine the fracture behavior of the nut. The critical crack length values which cause the fracture of the nut are determined under the different loading conditions.

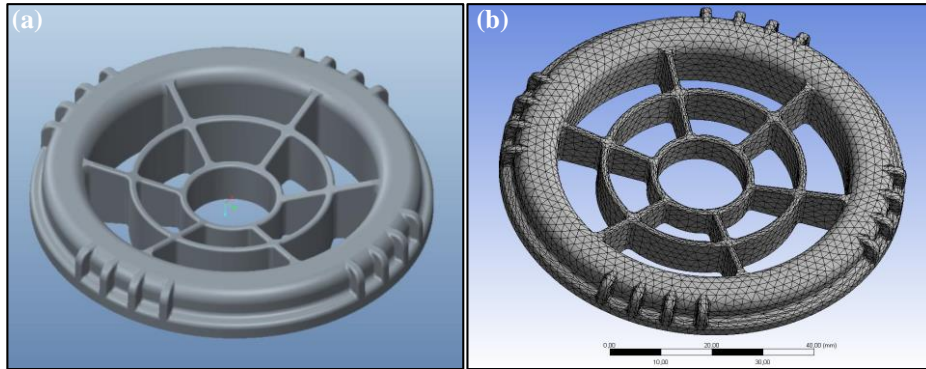


**Figure 4.** (a) Three dimensional solid and (b) finite element models of air break nut

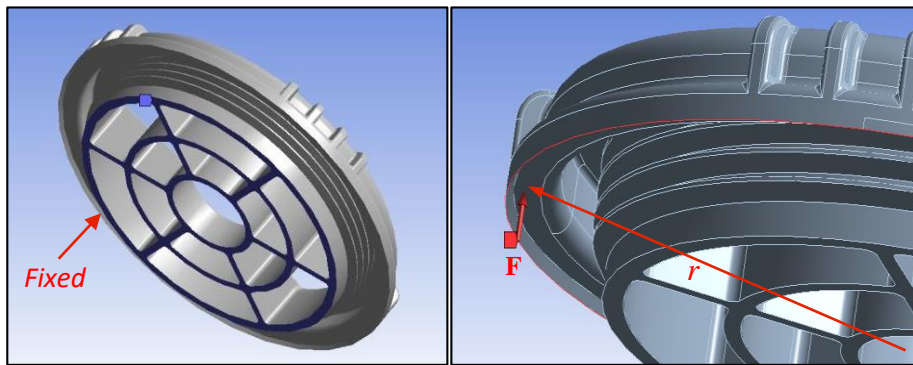


**Figure 5.** Boundary conditions

Figure 5 shows the boundary conditions of the air break nut in the finite element analyses. Air break nut is fixed from the back surfaces indicated by blue color. Force occurring during the assembly is perpendicular to the contact surface between the nut and tub. Value of this force is determined as  $F= 402.5$  N for the values of applied torque of  $T=16$  N-m and effective radius of  $r=39.75$  mm.

Table 1 presents the mechanical properties of PP T40, which is a type of polymers, used as the nut material. Polypropylene (PP) materials are used in various industrial areas mixing with some fillers such as minerals, clays and fibres [7]. Polypropylene is a semi-crystalline polymer having several disadvantages like brittleness, poor rigidity, molding shrinkage, poor high temperature creep. The addition of talc can improve the thermal deformation temperature,

the rigidity and increase the dimensional stability of products, and reduce the molding shrinkage of modified polypropylene [8, 9 ,10]. PPT 40 is polypropylene 40% talc filled material.

**Table 1.** Mechanical properties of PP T40 [6].

Mechanical property	Value	Units
Density	1.26	$g/cm^3$
Maximum Tensile Strength	$\geq 25$	MPa
Elongation	$\geq 3$	%
Young's modulus	$\geq 3250$	MPa
Fracture Toughness	$\geq 3$	$MPa\sqrt{m}$
Hardness	70-77	Shore-D



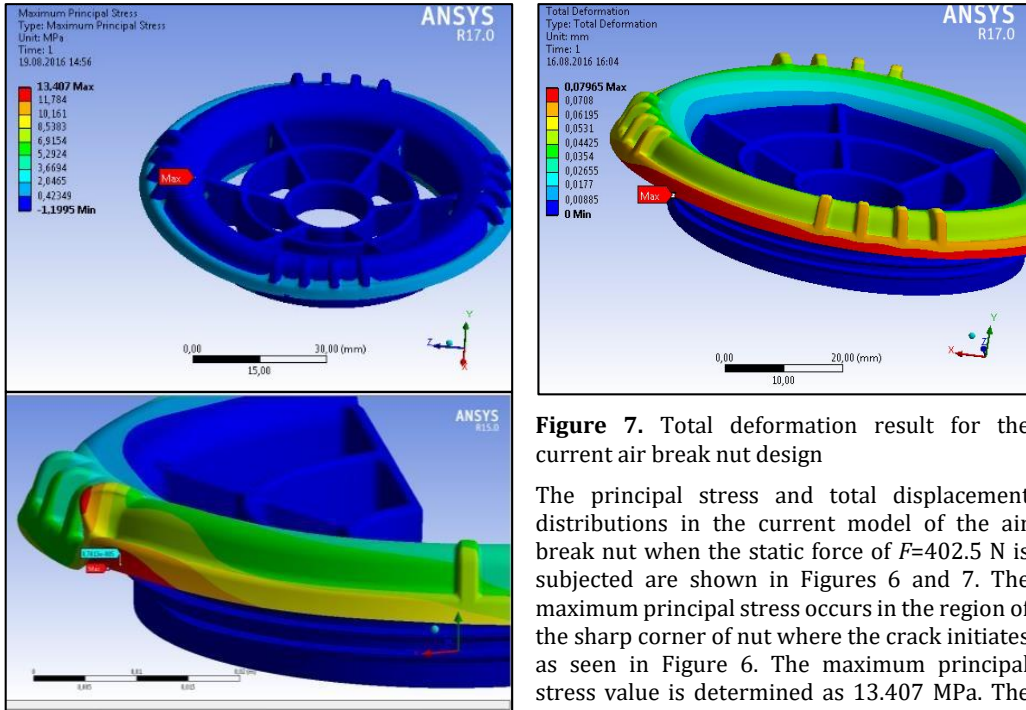


**Figure 6.** Principal stress distribution in the current air break nut

**Figure 7.** Total deformation result for the current air break nut design

The principal stress and total displacement distributions in the current model of the air break nut when the static force of  $F=402.5$  N is subjected are shown in Figures 6 and 7. The maximum principal stress occurs in the region of the sharp corner of nut where the crack initiates as seen in Figure 6. The maximum principal stress value is determined as 13.407 MPa. The maximum total displacement value is 0.0795 mm and occurs in the region where the force is applied as seen from Figure 7.

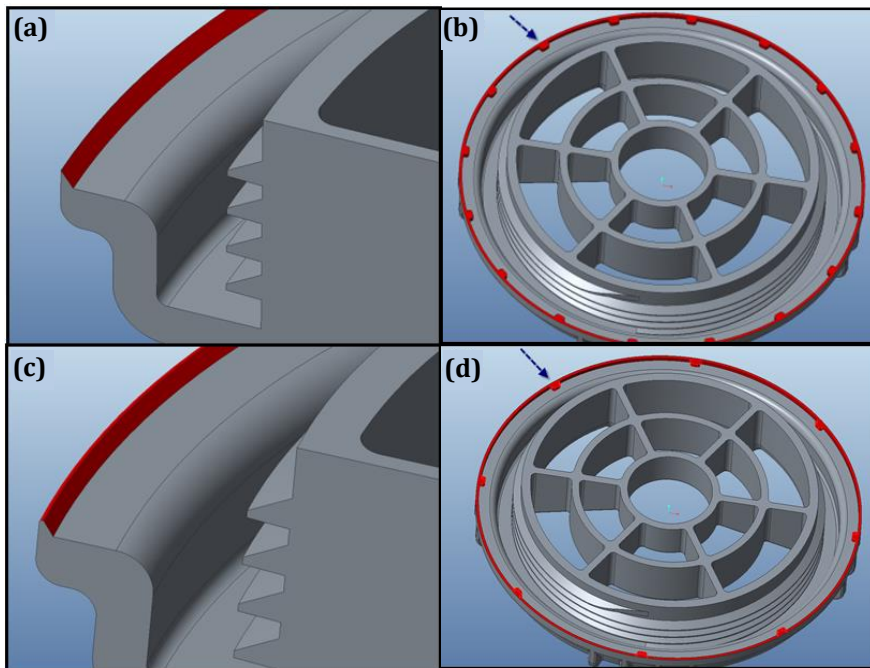


**Figure 8.** Alternative designs of the air break nut

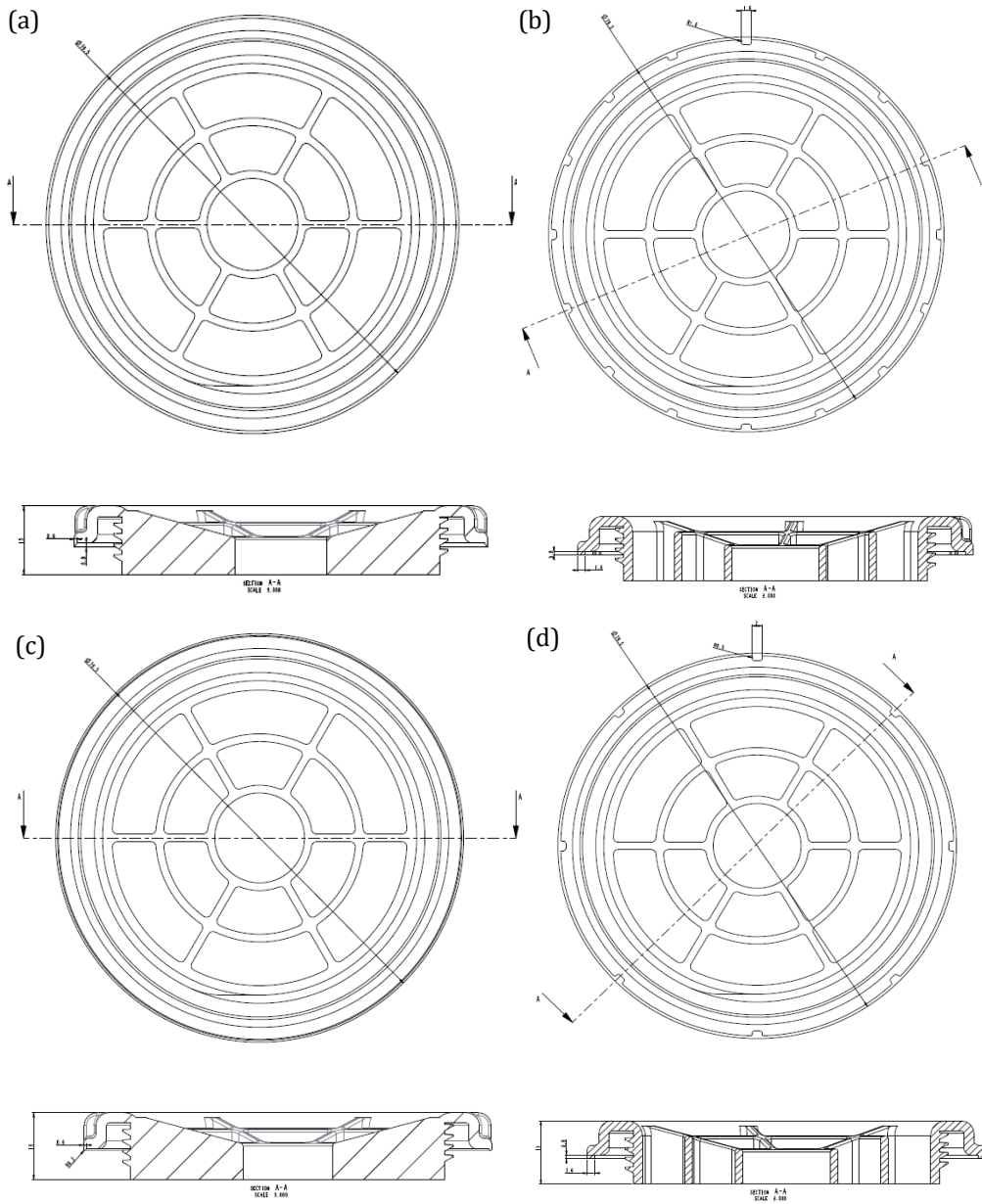


**Figure 9.** Technical drawings of alternative air break nut designs

#### 4. Alternative Air Break Nut Designs

In Figures 8 and 9, three dimensional solid models and technical drawings of the different air break nuts examined in this study are shown. Figure 8(a) shows the current nut model (Model A) having sharp corner which is used in mass production. In Figure 8(b), an alternative design to the current air break nut used in the mass

production is seen. This model is developed adding 16 strips on the sharp surfaces (Model B). Model in Figure 8(c) has a radius of 0.2 mm formed at the sharp-corner of Model A (Model C). Model in Figure 8(d) is reinforced adding eight strips in the region which is observed the fracture (Model D).

**5. Results**

In order to determine effect of the design on the fracture behavior of the air break nut, static structural and fracture analyses are carried out for each model mentioned in Section 4. Figure 10 shows the principal stress distributions in the alternative air break nut models. The minimum stress occurs when Model D having eight strips is used. In this model, the maximum principal stress value is 6.88 MPa.

As seen from the figures, the maximum principal stress occurring in Model C is determined as 9.94 MPa whereas the maximum principal stress value is approximately 9.52 MPa when Model B having 16 strips is used.

Figure 11 shows the displacement distributions in the different air break nut designs under the loading. As seen from the figures, the values of the total displacements are between 0.063-0.065 mm. The maximum displacement occurs in the present model.

When the results obtained from the structural analyses are evaluated, the maximum principal stress values for all models are smaller than the ultimate strength value of the PP T40 used as air break nut material. Based on these results, it may be considered that no damage will occur. However, fracture of the air break nuts may be occasionally experienced during assembly. In order to investigate the reason of this situation, it is necessary to carry out the fracture analyses of the nuts.

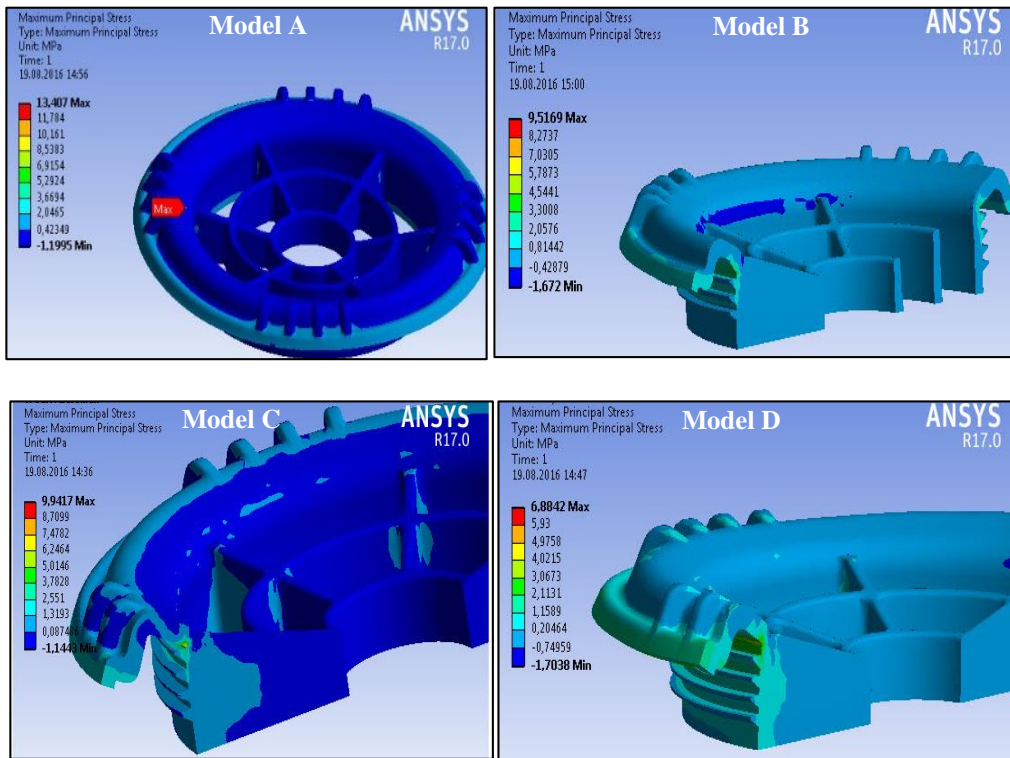


**Figure 10.** Maximum principal stress distributions in different air break nut models

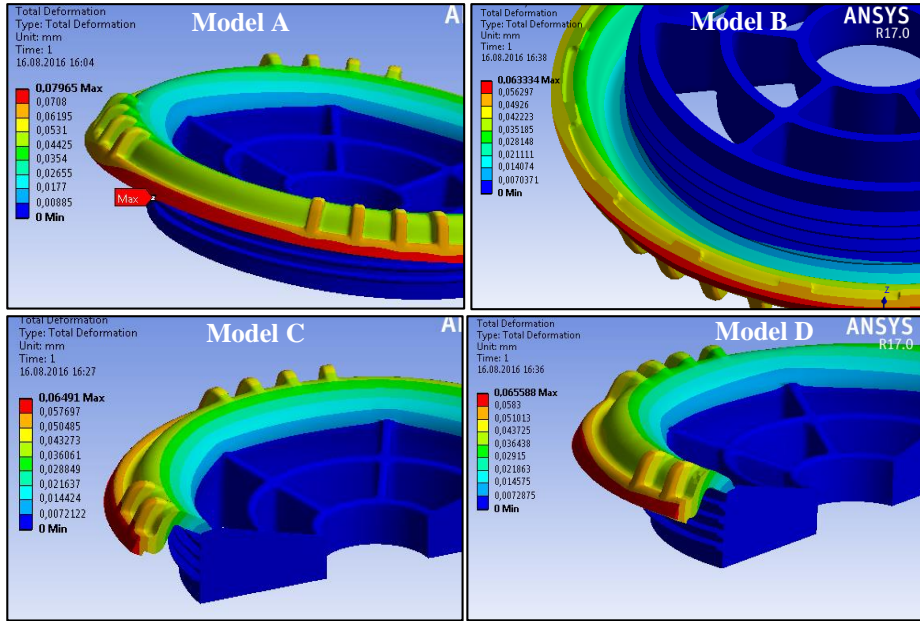


Figure 11. Displacement distributions in different air break nut models

As in the static analyses, fracture analyses are performed by ANSYS Workbench software. Because of the symmetry of the model, the 1/8 of air break nut is modeled to perform the fracture analyses. Solid model used in the fracture analysis can be seen in Figure 12.

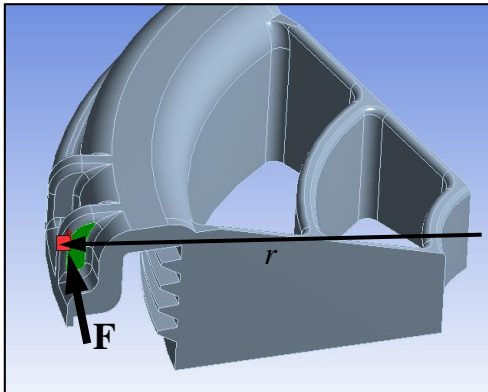


Figure 12. Solid model of the air break nut

The mesh of the crack region is shown in Figure 13. A semi-elliptical crack model which generally occurs in the structures is used in the numerical fracture analyses. Major and minor crack lengths of the crack are selected as 0.2 mm and 0.1 mm, respectively.

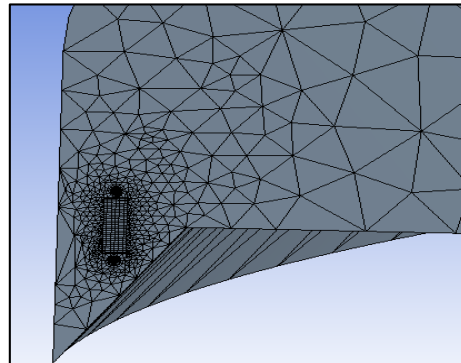


Figure 13. Finite element model of crack region

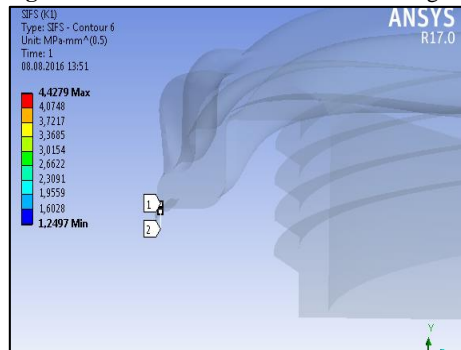


Figure 14. Stress intensity factor,  $K_I$



Figure 14 shows the stress intensity factor for Mode I (opening),  $K_I$ , obtained after the finite element analyses are performed for the current model. Stress intensity factor values for the current model subjected to the different load values can be seen in Table 2.  $K_I$ ,  $a_{major}$  and  $a_{minor}$ , which are given in Table 2 correspond to the stress intensity factor for Mode I, major crack length and minor crack length, respectively. Considering the results of stress intensity in Table 2, it is said that the fracture may occur if the current nut model has a 0.2 mm of crack length since the fracture toughness value of the material of the nut is  $3 \text{ MPa}\sqrt{\text{m}}$ . According to the Irwin criterion, a crack will begin to extend when the stress intensity factor,  $K_I$ , is increased to the fracture toughness of the material,  $K_{Ic}$  ( $K_I \geq K_{Ic}$ )

[11]. If the calculated force value, 402.5 N, is applied, it is clear that fracture occurs since the corresponding stress intensity factor,  $K_I$ , is largely greater than the fracture toughness value of nut material,  $K_{Ic}=3 \text{ MPa}\sqrt{\text{m}}$ .

Table 3 shows the stress intensity factors obtained for the nut model with ribbon tiers, Model C, that is considered under the different loading conditions. As seen from the table, crack length, 0.2 mm, becomes critical in case of present loading condition, 402.5 N.

Table 4 presents the maximum principal stress, maximum displacement, critical crack length values for Models A and C subjected to the critical force and torque.

**Table 2.** Stress intensity factor results for different applied force in current design.

Applied Force (N)	Material	$a_{major}$ (mm)	$a_{minor}$ (mm)	$K_I$ $\text{MPa}\sqrt{\text{m}}$
100	PP T40	0.2	0.1	2.43
200	PP T40	0.2	0.1	3.06
300	PP T40	0.2	0.1	3.71
<b>402.5</b>	<b>PP T40</b>	<b>0.2</b>	<b>0.1</b>	<b>4.42</b>
450	PP T40	0.2	0.1	4.76
600	PP T40	0.2	0.1	5.83

**Table 3.** Stress intensity factor values for different applied force for Model C.

Applied Force (N)	Material	$a_{major}$ (mm)	$a_{minor}$ (mm)	$K_I$ $\text{MPa}\sqrt{\text{m}}$
100	PP T40	0.2	0.1	1.22
200	PP T40	0.2	0.1	1.75
300	PP T40	0.2	0.1	2.39
<b>402.5</b>	<b>PP T40</b>	<b>0.2</b>	<b>0.1</b>	<b>3.07</b>
450	PP T40	0.2	0.1	3,39
600	PP T40	0.2	0.1	4.41

It can be clearly seen from the table that the maximum principle stress and maximum displacement values are decreased when the new design of the nut is used. In terms of the fracture behavior, improving the nut design results in decrease of  $K_I$  from  $4.42 \text{ MPa}\sqrt{\text{m}}$  to

$3.07 \text{ MPa}\sqrt{\text{m}}$  and thus increase of critical crack length. All these results prove that the new model is tougher than the currently used model against to the fracture.

**Table 4.** Comparison of the result for current model and Model C.

Calculated Values	Unit	Current Design	Model C
$\sigma_{\max}$	MPa	13.4	9.94
$\delta_{\max}$	mm	0.079	0.064
$K_I$	$\text{MPa}\sqrt{\text{m}}$	4.42	3.07
$a_{\text{cr}}$	mm	0.075	0.2
$F_{\text{cr}}$	N	402.5	402.5
$T_{\text{cr}}$	N-m	16	16

## 6. Conclusions

The scope of this study is to examine the probable reasons which cause to the cracking of the nut when the nut is assembled to the dishwasher. These reasons are listed as:

Some of the operators may not use correctly the apparatus during the assembly process (Greater force than the required force may be applied to the nut).

The current design which has been improved considering resistance against to the corrosion has the sharp edges. So, fracture of the air break nut may be due to the design. It is predicted that the sharp edges cause to propagate of the crack which is probably present.

Air break nut which is used in dishwasher has properties of brittle material. Its fracture toughness is low. Instead of using polypropylene which is a brittle material, fracture resistant materials having high fracture toughness for the current design can be used.

Another reason may be the piece in injection molding machines or mold problems (unable to supply enough material, not enough tonnage of the injection molding machine, insufficient pressing time of the part in injection molding machine).

In the light of the results obtained in this study, new mold can be made for different design or it can be made modification to current mold.

## References

- [1] Sun, C.T., Jin, Z.H. 2012. Fracture Mechanics. ELSEVIER; ISBN:978-0-12-385001-0.
- [2] Kubiak, Sz. J., Segura, J.A., Gonzalez, G.R., García, J.C., Sierra, F.E., Nebradt, J.G., Rodriguez, J.A. 2009. Failure analysis of the 350MW steam turbine blade root, Engineering Failure Analysis, 16(4), pp. 1270 – 1281.
- [3] Urquiza, G., Garcia, J.C., Gonzalez, J.G., Castro, L., Rodriguez, J.A., Basurto-Pensado, M.A., Mendoza, O.F. 2014. Failure analysis of a hydraulic Kaplan turbine shaft, Engineering Failure Analysis, 41, pp. 108 – 117.
- [4] Karalis, D.G., Melanitis, N.E., Yannoulis, Y.G. Failure analysis of a Cue12Mn mechanical fastener in marine environment, Engineering Failure Analysis, 94, pp. 69 – 77.
- [5] ANSYS Workbench R.17 User's Manual.
- [6] Ashby, M.F., Jones, D.R.H. 1980. Engineering Materials-An Introduction to Their Properties and Applications, Pergamon Press Inc, Elmsford.
- [7] Gu, F., Hall, P., Miles, N.J. 2015. Experimental Investigating Effect of Reprocessing on Properties of Composites based on Recycled Polypropylene, International Conference on Polypropylene, International Conference on Power Electronics and Energy Engineering (PEEE 2015), 177-184.
- [8] Chen Q., Yu, R.B. 2018. Effect of Talc on High-temperature Exothermic Peak and Properties of Polypropylene International Conference on Computer

Information and Automation Engineering, IOP Conf. Series: Materials Science and Engineering, 359. DOI:10.1088/1757-899X/359/1/012031.

[9] Parija, S., Nayak, S.K., Verma, S.K., Tripathy, S. S. 2010. Studies on physico-mechanical properties and thermal characteristics of polypropylene/layered silicate nanocomposites Polymer Composites, 25, pp. 646-52, <https://doi.org/10.1002/pc.20059>.

[10] Zheng, C., Liu, J., Fan, J., Luan, Y., Song, L. 2016. Research on deformation behavior of isotactic polypropylene in uniaxial geogrid manufacture, Materials & Design, 91, pp. 1-10.

[11] Freund, L.B. 1990. Dynamic Fracture Mechanics. Cambridge University Press; ISBN: 9780511546761.